Photochemistry of Di(deoxyribonucleoside) Methylphosphonates Containing N^3-Methyl-4-thiothymine

Pascale Clivio and Jean-Louis Fourrey*

Institut de Chimie des Substances Naturelles, CNRS, F-91198 Gif sur Yvette Cedex, France

Tomas Szabó and Jacek Stawinski*

Department of Organic Chemistry, University of Stockholm, S-106 91 Stockholm, Sweden

Received June 15, 1994[⊗]

(*Rp*)- and (*Sp*)-5′-N^3-methyl-4-thiothymidine 3′-(thymidinyl methylphosphonate) (T*p*m^{3}s^{4}T) (**11a** and **11b**), respectively, have been synthesized in order to elucidate their photochemical behavior in comparison with that of their phosphate congener **1b**. The dinucleoside methylphosphonates proved to be less rapidly photolyzed than **1b** and gave more photoproducts. The structure and stereochemistry of each photoproduct were determined by NMR studies. A plausible mechanism to explain the formation of the major photoproducts has been proposed. It involves two pathways: either cycloaddition or radical coupling. The former one led to thietane derivatives, the formation of which is of relevance to the mechanism to give (6–4) bipyrimidine photoproducts in DNA. Most of the other photoproducts were probably formed from a biradical generated via hydrogen abstraction from the C5 methyl of the T*p*- part of each dimer. Compounds **15** which represent a new type of photoproduct in the nucleic acid series are most likely formed by this route. Another significant finding of this study was that the *Rp* dinucleoside methylphosphonate (**11a**) is a better mimic of the phosphate backbone, as found in DNA, than its *Sp* diastereomers (**11b**).

Introduction

The antisense approach for specific gene inhibition is currently receiving a great deal of attention.[1] In this domain, the use of unmodified oligonucleotides has been limited by several factors such as susceptibility to nucleases digestion and poor cell penetration. To circumvent these problems methylphosphonate oligonucleotide analogs have been designed. Such nonionic constructions exhibit reasonable passive cell membrane penetration as well as strong nuclease resistance. Moreover, they form stable hybrids with a complementary DNA (or RNA) strand although the effects of the *P*-methyl group on helix formation have not yet been fully elucidated.[2]

It is generally accepted that the stereochemistry of the phosphorus atom might have an influence on several factors governing the geometry of the modified diester backbone such as the hydration pattern and electrostatic interactions.[3] Thus, oligonucleotide methylphosphonates with predominantly *Rp* configuration have been considered to afford more stable hybrids with complementary DNA than their *Sp* analogs.[4] For a number of related investigations, di(deoxyribonucleotides) and their analogs have served as model systems either to predict conformational modifications produced by the incorporation of a modified deoxynucleoside in DNA or to study DNA reactivity. In this respect, the conformation of several dinucleoside methylphosphonates has been studied to get an insight into the conformational state of methylphosphonate-containing oligonucleotides. *Rp* configurated dinucleoside methylphosphonate isomers were found to better mimic dinucleoside phosphates than *Sp* isomers.[4b,5] Similarly, various dinucleoside phosphates have been used to study the mechanism of cyclobutane or (6-4) pyrimidine–pyrimidone photoproduct formation which are responsible for major photolesions in DNA.[6] Recently, a model system based on the photochemistry of the dinucleoside phosphate **1a** (Tps^{4}T) has been designed to study the mechanism of formation of (6-4) lesions in DNA.[7] Thymidylyl-(3′–5′)-4-thiothymidine (**1a**) is an analog of thymidylyl-(3′–5′)-thymidine (TpT) in which thymidine at the 3′-position is replaced by the selectively photoreactive 4-thiothymidine. In contrast to TpT, irradiation of **1a** did not lead to cyclobutane dimers but provided in satisfactory yield (6–4) bipyrimidine photoproducts as well as another type of product arising from the generation of a radical at the methyl position of thymidine at the 5′-end. Altogether, these observations could be conveniently interpreted on the basis of earlier photochemical studies which demonstrated that the

[⊗] Abstract published in *Advance ACS Abstracts,* October 15, 1994.

(1) (a) Uhlmann, E.; Peyman, A. *Chem. Rev.* **1990**, *90*, 544–579. (b) Crooke, S. T. *Annual. Rev. Pharmacol. Toxicol.* **1992**, *32*, 329–376. (c) *Gene Regulation: Biology of Antisense RNA and DNA*; Erickson, R. P., Izant, J. G., Eds.; Raven Press: New York, 1992. (d) Milligan, J. F.; Matteucci, M. D.; Martin, J. C. *J. Med. Chem.* **1993**, *36*, 1923–1937. (d) Beaucage, S. L.; Iyer, R. P. *Tetrahedron* **1993**, *49*, 6123–6194. (e) Varma, R. S. *Synthesis* **1993**, 340–346.

(2) (a) Miller, P. S *Bio/Technology* **1991**, *9*, 358–362. (b) Lesnikowski, Z. J. *Bioorg. Chem.* **1993**, *21*, 127–155.

(3) (a) Hausheer, F. H.; Chandra Singh, U.; Palmer, T. C.; Saxe, J. D. *J. Am. Chem. Soc.* **1990**, *112*, 9468–9474. (b) Hausheer, F. H.; Rao, B. G.; Saxe, J. D.; Singh, U. C. *Ibid.* **1992**, *114*, 3201–3206.

(4) (a) Lesnikowski, Z. J.; Jaworska, M.; Stec, W. J. *Nucleic Acids Res.* **1990**, *18*, 2109–2115. (b) Samstag, W.; Engels, J. W. *Angew. Chem., Int. Ed. Engl.* **1992**, *31*, 1386–1388.

(5) (a) Miller, P. S.; Yano, J.; Yano, E.; Carroll, C.; Jayaraman, K.; Ts'o, P. O. P. *Biochemistry* **1979**, *23*, 5134–5143. (b) Kan, L. S.; Cheng, D. M.; Miller, P. S.; Yano, J.; Ts'o, P. O. P. *Ibid.* **1980**, *19*, 2122–2132. (c) Swarna Latha, Y.; Yathindra, N. *J. Biomol. Struct. Dyn.* **1991**, *9*, 613–631.

(6) (a) Cadet, J.; Vigny, P. *The Photochemistry of Nucleic Acids*; Morrison, H., Ed.; Wiley and Sons: New York, 1990; Vol. 1, p 79. (b) Koning, T. M. G.; Van Soest, J. J. G.; Kaptein, R. *Eur. J. Biochem.* **1991**, *195*, 29–40. (c) Douki, T.; Voituriez, L.; Cadet, J. *Photochem. Photobiol.* **1991**, *53*, 293–297. (d) Kan, L.-S.; Voituriez, L.; Cadet, J. *J. Photochem. Photobiol. B: Biol.* **1992**, *12*, 339–357. (e) Douki, T.; Cadet, J. *J. Photochem. Photobiol., B: Biol.* **1992**, *15*, 199–213. (f) Kao, J. L.-F.; Nadji, S.; Taylor, J.-S. *Chem. Res. Toxicol.* **1993**, *6*, 561–567. (g) Tabaczynski, W. A.; Lemaire, D. G. E.; Ruzsicska, B. P.; Alderfer, J. L. *Biopolymers* **1993**, *33*, 1365–1375. (h) Lemaire, D. G. E.; Ruzsicska, B. P. *Photochem. Photobiol.* **1993**, *57*, 755–769.

(7) Clivio, P.; Fourrey, J.-L.; Gasche, J.; Favre, A. *J. Am. Chem. Soc.* **1991**, *113*, 5481–5483.

0022-3263/94/1959-7273$04.50/0

Scheme 1

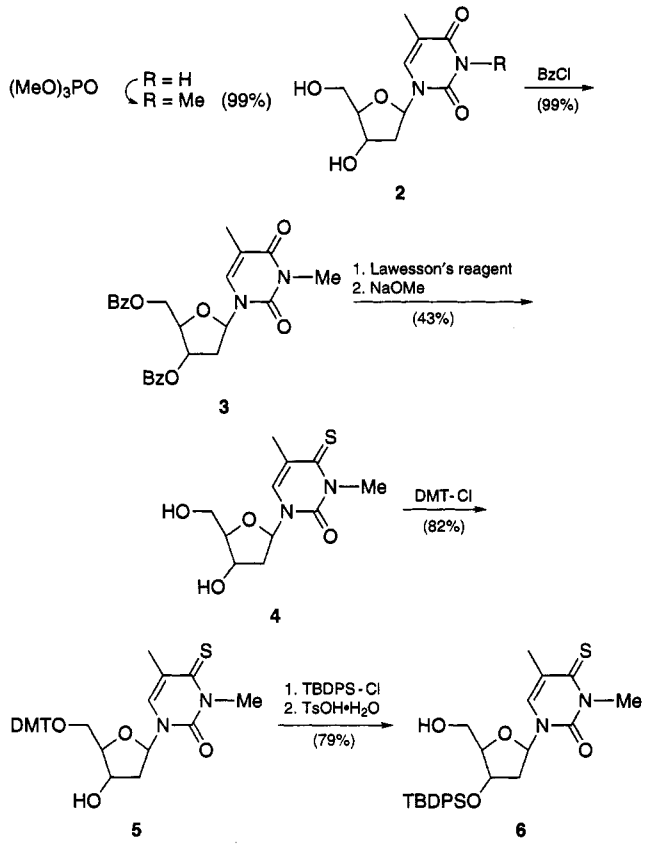

Scheme 2

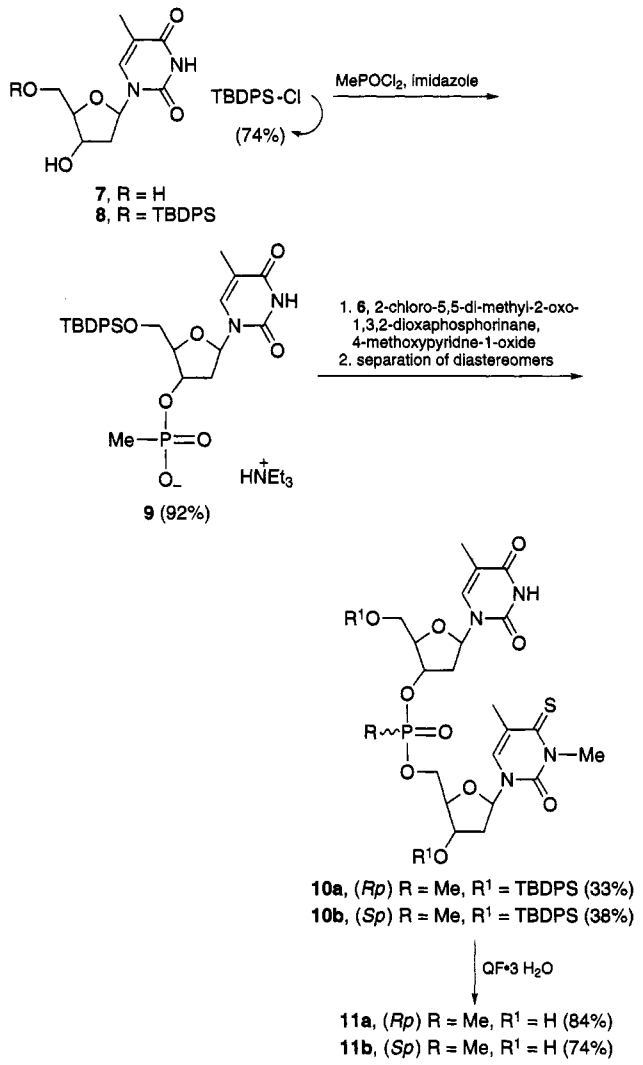

4-thiouracil system undergoes two types of light-induced reactions: cycloaddition and radical reactions.[8]

Herein, we proposed to probe, at the dinucleotide level, how in the methylphosphonate series, the conformational mobility could be influenced by the presence and the chirality of the *P*-methyl group. On the basis of our earlier studies, we have prepared and examined the photochemistry of (*Rp*)- and (*Sp*)-5′-N^3-methyl-4-thiothymidine 3′-(thymidinyl methylphosphonate) (**11a** and **11b**) (Tpm^{3}s^{4}T), respectively, having a N^3-methyl-4-thiothymine residue at the 3′-end. The results were compared with those previously obtained for thymidylyl(3′-5′)-N^3-methyl-4-thiothymidine (Tpm^{3}s^{4}T) (**1b**).[9a,10] N^3-Methylated compounds were chosen because, in contrast to their N^3-unsubstituted analogs, they can give rise to stable and conformationally rigid thietanes, the formation of which might reveal some structural characteristics of their precursors.

Results and Discussion

Synthesis and Photolysis of Di(deoxyribonucleoside) Methylphosphonates (*Rp*)-11a and (*Sp*)-11b. The synthesis of thiosubstituted dinucleoside methylphosphonates **11a** and **11b** is outlined in Schemes 1 and 2. The N^3-methyl-4-thiothymidine unit **6** was prepared according to literature procedures or modifications thereof.[10] Thus, **6** was obtained by tritylation of the primary hydroxyl function in **4** followed by silylation with *tert*-butyldiphenylsilyl chloride (TBDPS-Cl) and removal of the trityl group. The 3′-(methylphosphonate) **9** was prepared by reaction of 5′-*O*-(*tert*-butyldiphenylsilyl)-thymidine (**8**)[11] with methylphosphonic bis(imidazolide)[12] followed by hydrolysis.

Condensation of **9** with **6** was effected by the 2-chloro-5,5-dimethyl-2-oxo-1,3,2-dioxaphosphinane/4-methoxypyridine 1-oxide reagent system.[13] Separation of diastereomers using semipreparative HPLC on silica gel followed by desilylation afforded optically pure dinucleoside methylphosphonates **11a** and **11b**. X-ray analysis of crystals grown from a dilute methanolic solution of diastereomer **11b**,[14] obtained from the deprotection of the slower eluting *bis* silylated diastereomer **10b**, identified the absolute configuration at the phosphorus center of this compound as *Sp*. Notable are the ^{31}P NMR chemical shifts and chromatographic mobilities of the *Rp* and *Sp* diastereomers **11a** and **11b**. They are consistent with an experimental rule[15] correlating these properties with absolute configuration at the phosphorus center.

(8) (a) Fourrey, J.-L.; Jouin, P. *Tetrahedron Lett.* **1973**, 3225–3227. (b) Fourrey, J.-L.; Jouin, P.; Moron, J. *Ibid.* **1974**, 3005–3006. (c) Fourrey, J.-L. *Ibid.* **1976**, 297–300.

(9) (a) Clivio, P.; Fourrey, J.-L.; Gasche, J.; Favre, A. *Tetrahedron Lett.* **1992**, *33*, 1615–1618. (b) The exact molecular weight of **14a** was definitively established by electrospray MS which led us to revise our initial interpretation of the FABMS.[9a]

(10) Clivio, P.; Fourrey, J.-L.; Gasche, J.; Favre, A. *J. Chem. Soc., Perkin Trans. 1* **1992**, 2383–2388.

(11) Matulic-Adamic, J.; Watanabe, K. A. *Chem. Scripta* **1986**, *26*, 127–134.

(12) Miller, P. S.; Reddy, M. P.; Murakami, A.; Blake, K. R.; Lin, S.-B.; Agris, C. H. *Biochemistry* **1986**, *25*, 5092–5097.

(13) Stawinski, J.; Strömberg, R.; Szabó, T. *Nucleic Acids Res., Symp. Ser.* **1991**, *24*, 229.

(14) Szabó, T.; Carlsson, S.; Norrestam, R.; Stawinski, J. Manuscript in preparation.

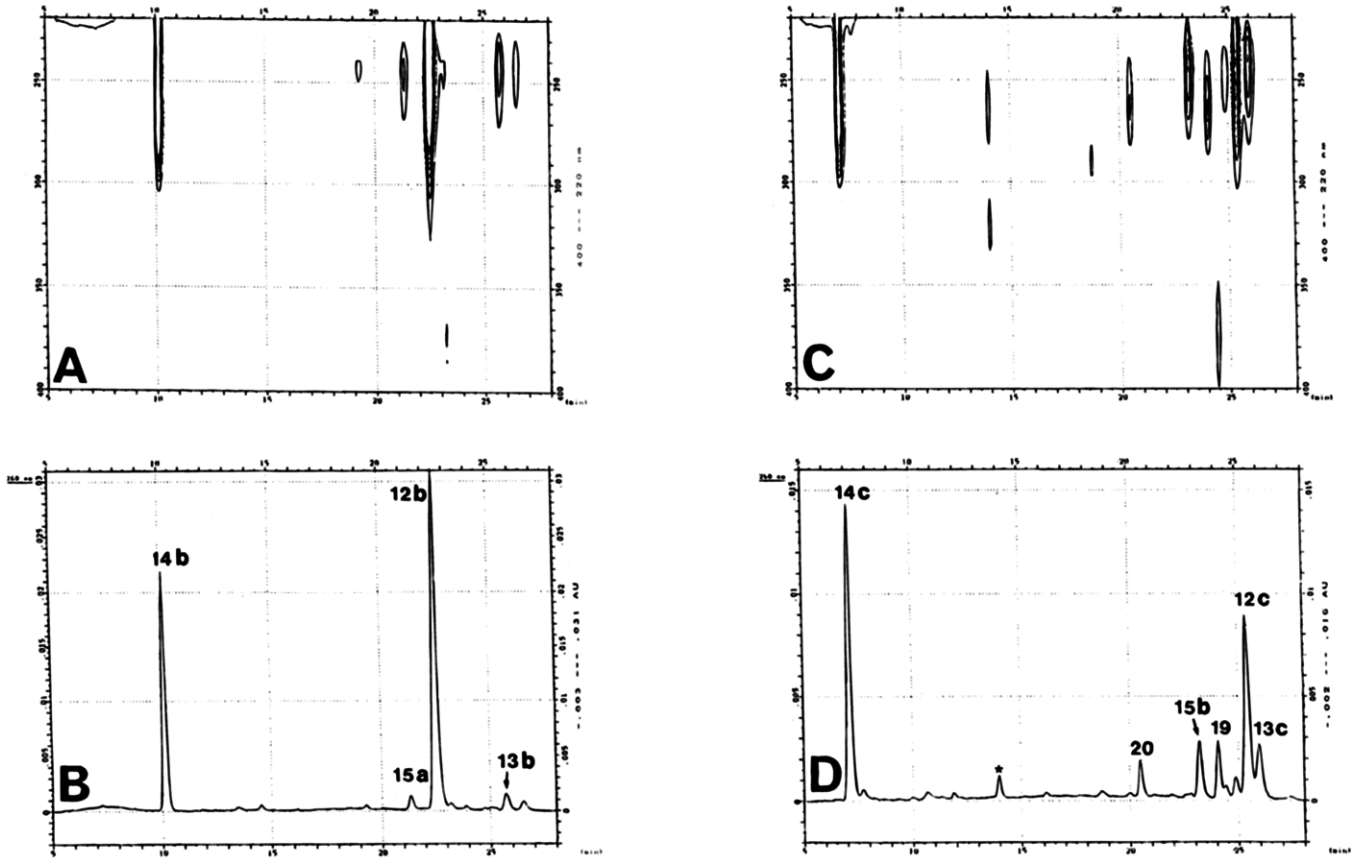

Figure 1. A and C: 2D-chromatograms (t_R, retention time (min) *versus* UV absorption (nm)) after 3 h 10 min photolysis of **11a** and **11b**, respectively. B and D: corresponding chromatograms monitored at 260 nm. *Unidentified compound which gave after the desalting step compounds **17** and **18**.

Table 1. Reversed Phase HPLC Separation[a] of Photoproducts (%) Obtained after Irradiation of 1b,[9a] 11a, and 11b and Recovery of Starting Material Retention Times (min)

product	1b	12a	13a	14a	11a	12b	13b	14b	15a	11b	12c	13c	14c	15b	19	20
yield, %	4	25	2	24	5	5.6	0.7	6.4	2.1	5	4.8	0.6	3.0	4.6	1.4	0.5
t_R (min)	51.9	32.3	39.5	11.5	45.4	22.5	25.1	9.9	20.7	46.9	25.1	25.6	6.8[b]	22.7	23.8	20.1

[a] For HPLC conditions, see Experimental Section. [b] 5.7 and 0.6% of hydrolyzed products **17** and **18**, respectively, were also isolated.

The choice in the synthetic strategy of the highly lipophilic TBDPS group, removable under mild, neutral conditions, served three main purposes: (i) it minimized the number of synthetic steps, (ii) secured integrity of the internucleotidic bond during the deprotection, and (iii) facilitated an otherwise usually difficult separation of the individual diastereomers of **11a** and **11b**.

The two methylphosphonate derivatives **11a** and **11b** were subjected to photolysis upon 360 nm irradiation in aqueous solution. The progress of the reaction was monitored by the decrease of the ratio of the two UV absorption maxima at 330 and 267 nm. Compared to dinucleoside phosphate **1b**, these methylphosphonates were less rapidly photolyzed (under the same conditions of irradiation of **1b** the ratio of the two maxima reached after 10 h a value of 0.27, while for the methylphosphonates **11a** (*Rp*) and **11b** (*Sp*) the corresponding ratios were 0.4 and 0.6, respectively, after 16 h). An HPLC chromatogram, monitored at 260 nm, together with the 2D plot of each irradiated isomer are shown in Figure 1. By comparison of these chromatograms it became apparent that the *Sp* isomer **11b** gives rise to more photoproducts than the *Rp* isomer (**11a**). Four photoproducts **12b**, **13b**, **14b**, and **15a** have been isolated from irradiated *Rp* methylphosphonate isomer **11a**, whereas eight photoproducts **12c**, **13c**, **14c**, **15b**, and **17**–**20** have been isolated from the irradiation mixture of the *Sp* methylphosphonate **11b** (Chart 1).

Thietanes **12b** and **13b** in the *Rp* series and compounds **12c** and **13c** in the *Sp* series, as well as photoproducts having a methylene bridge between the two pyrimidines such as (*Rp*)-**14b** and (*Sp*)-**14c**, are reminiscent of their corresponding analogs formed under the same irradiation conditions in the phosphate series (**1b**), *i.e.*, (a) cycloaddition between the thiocarbonyl group of the 3′-base and the C5–C6 double bond of the 5′-base both in the anti glycosyl conformation leading to **12a** or with the 5′-base and the 3′-base in syn and anti glycosyl conformation, respectively, leading to **13a** and (b) generation of a methylene radical from the methyl of the 5′-anti base followed by addition of the latter to the thiol-substituted C4-radical of the 3′-anti base leading to **14a**.

This indicates that the *Rp* and *Sp* dinucleoside methylphosphonates **11a** and **11b** are able to produce the same photoproducts as the phosphate analog **1b** albeit in lower yields (Table 1). However additional compounds **15a** and **15b**, not isolated in the phosphate series, were

(15) Vyazovkina, E. V.; Engels, I. W.; Lebedev, A. V. *Bioorg. Khim.* **1993**, *19*, 197–210.

Chart 1

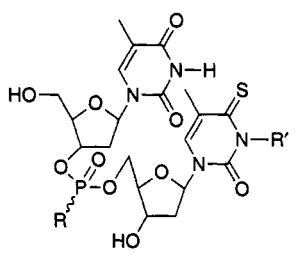

1a, R = OH; R′ = H
1b, R = OH; R′ = Me
11a (*Rp*), R = R′ = Me
11b (*Sp*), R = R′ = Me

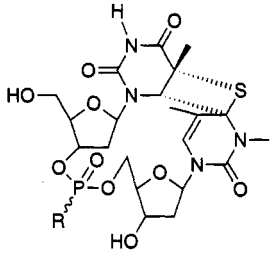

12a, R = OH
12b, (*Rp*), R = Me
12c, (*Sp*), R = Me

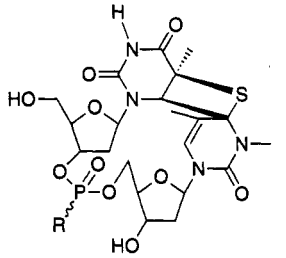

13a, R = OH
13b, (*Rp*), R = Me
13c, (*Sp*), R = Me

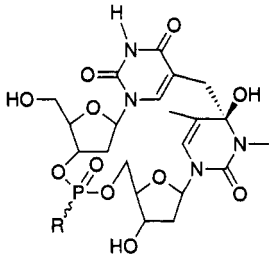

14a, R = OH
14b, (*Rp*), R = Me
14c, (*Sp*), R = Me

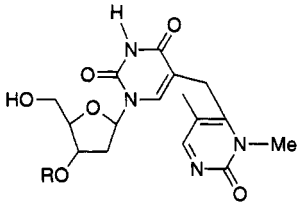

17, R = H
18, R = P(O)(Me)OH

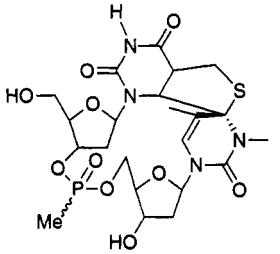

15a, (*Rp*), C5 *R*; C6*R*
15b, (*Sp*), C5 *S*; C6*S*

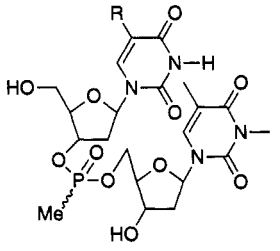

19 (*Sp*), R = Me
20 (*Sp*), R = CH_2OH

produced during irradiation of both methylphosphonates **11a** and **11b**. They resulted apparently from a novel pathway involving the same biradical intermediate as in the formation of either (*Rp*)-**14b** or (*Sp*)-**14c** (Scheme 3). In this case, coupling occurred between position C4 of the 3′-base with position C6 of the 5′-base, leading to an exocyclic unsaturated carbonyl system, the proximal C4 thiol nucleophile of which underwent Michael addition to give **15a** and **15b**, respectively. It is worthy of note that the stereochemical pathways leading to **15a** and **15b** are different; thus, **15a** resulted from a radical coupling with the two bases in the anti glycosyl conformation whereas for **15b** the 5′-base and the 3′-base were syn and anti oriented, respectively.

The absolute configuration at the phosphorus center apparently influences the stability of photoproducts **14b** and **14c**. Thus, from **14c**, compounds **17** and **18**, resulting from the hydrolysis of the 3′-end *N*-glycosidic bond,

Scheme 3

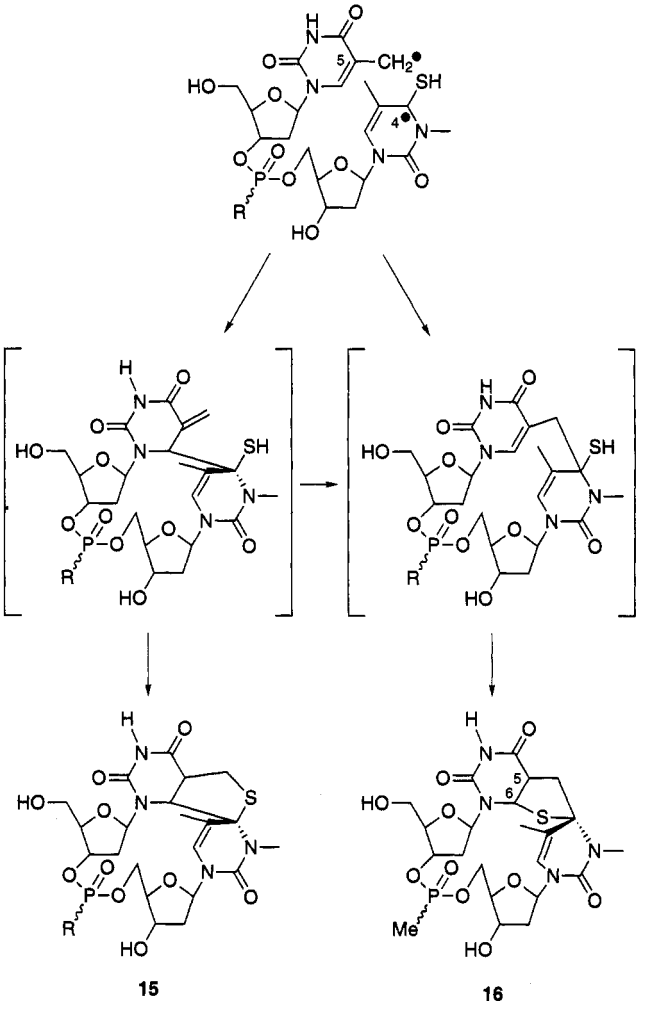

were formed in contradistinction to **14b** which seemed to be hydrolytically stable.

Interestingly, photolysis of (*Sp*)-**11b** produced also two additional compounds **19** and **20** which resulted from an oxidative process.

Structural Analysis. For the sake of convenience, the photoproducts which differ only in stereochemistry at designated chiral centers will be discussed together during their structural analysis.

Photoproducts 12b–c and 13b–c. The FABMS (positive mode) of compounds **12b**, **12c**, **13b**, and **13c** were characterized by the presence of a peak at *m/z* 597 $(M + Na)^+$, indicating that they had the same molecular weight as the starting material **11a** and **11b**. The ^1H and ^{13}C NMR spectra of compounds **12b** and **12c** (Tables 2 and 3) were quite similar to those of the known thietane **12a** allowing a straightforward identification of all the signals.[9a,16] Moreover, configurations of the asymmetric centers of the two bases of **12b** and **12c**, assigned from 2D phase sensitive NOESY spectra (Table 4), were identical to those of **12a**;[9a] thus, carbons C5 and C6 of the T*p*- base were both in the *R* configuration and that at C4 of the -*p*T base was in the *S* configuration.

(16) Assignment of the NMR signals of **12a** was performed by $^{13}C-^1H$ COSY and long range $^{13}C-^1H$ COSY experiments. The long range $^{13}C-^1H$ COSY spectrum gave the following sets of correlation: T*p*-H6 – T*p*-C4 (^3J); T*p*-H6 – T*p*-C5 (^2J); T*p*-C6 – T*p*-CH_3 (^3J); T*p*-C4 – -*pTCH*$_3$ (^3J); -*p*TH6 – -*p*TC4 (^3J); -*p*TH6 – -*p*TC2 (^3J); -*p*TC2 – N^3-CH_3 (^3J), -*p*TC4 – N^3-CH_3 (^3J), -*p*TCH_3 – -*p*TC5 (^2J), -*p*TCH_3 – -*p*TC4 (^3J).

Table 2. ^{1}H NMR Chemical Shift Data for the Thietanes 12a–c and 13a–c in D_2O

	Tp–						–pT					
proton	**12a**	**12b**	**12c**	**13a**	**13b**	**13c**	**12a**	**12b**	**12c**	**13a**	**13b**	**13c**
H1′	6.31	6.33	6.22	5.09	4.93	5.36	6.33	6.35	6.22	6.22	6.30	6.18
H2′	2.00	1.97	2.14	2.47	2.65[a]	2.20	2.55	2.48	2.46	2.47	2.43	2.46
H2″	2.40	2.48	2.46	2.78	2.88[a]	2.75	2.25	2.23	2.34	2.27	2.23	2.32
H3′	4.60	4.92	4.60	4.66	4.80	4.95	4.69	4.54	4.60	4.47	4.40	4.32
H4′	3.81	3.90	3.96	4.14	4.10	4.32	3.96	4.00	3.96	3.88	3.95	3.95
H5′	3.78	3.75	3.74	3.76	3.74	3.70	3.92	4.15	4.21	3.88	4.10	3.95
H5″	3.86	3.85	3.86	3.76	3.74	3.70	3.92	4.15	4.21	4.06	4.25	4.32
H6	4.97	5.02	4.99	5.18	5.12	5.20	6.44	6.40	6.42	6.48	6.47	6.40
CH_3	1.83	1.82	1.82	1.94	1.92	1.89	2.24	2.23	2.24	2.04	2.01	2.03
NCH_3							3.34	3.33	3.31	3.47	3.46	3.43
p-CH_3		1.67	1.75		1.64	1.65						

[a] Assigned from comparison with those of **13a** and **13c** since Tp-H1′ and Tp-H3′ signals were overlapped and Tp-H6 proton was syn.

Table 3: ^{13}C NMR Chemical Shift Data for 1b, 11a–b, 12a–c, and 14a–c in D_2O

carbon	**1b**[10]	**11a**[a]	**11b**[a]	**14a**	**14b**	**14c**	**12a**	**12b**	**12c**
Tp-C2	152.5[b]	152.2[b]	150.4[b]	152.1	153.1[b]	153.8[b]	154.7	155.9[b]	155.0[b]
Tp-C4	167.3	166.2	163.6	166.0	167.0	166.6	176.4	177.7	177.0
Tp-C5	112.6	111.8	109.7	110.0	112.2[c]	111.0[c]	43.6	44.5	43.2
Tp-C6	138.5	137.7	135.8	141.0	141.7	140.3	68.2	69.1	68.6[c]
Tp-CH_3	13.1	12.5	12.2	30.6	31.7	30.9[d]	25.7	26.8	25.8
Tp-C1′	86.4	86.0	83.6	84.1	85.2	84.0	84.0	84.8	84.7
Tp-C2′	39.1	39.8	37.7	39.9	40.6	39.9[e]	36.5	37.6[c]	36.3[d]
Tp-C3′	76.4	78.1	75.8	71.3	70.9	71.9	73.0	73.6	75.4
Tp-C4′	87.0[c]	87.3[c]	85.2[c]	85.2	85.7[d]	84.0	85.0	85.1[d]	83.6[e]
Tp-C5′	62.3	62.4	60.8	59.7	59.9	58.1	60.4	61.2	60.0
-pTC2	150.9[b]	150.4[b]	148.4[b]	153.9	154.9[b]	152.7[b]	154.7	155.8[b]	154.6[b]
-pTC4	192.2	192.5	190.4	89.3	90.1	88.9	79.5	80.2	78.9
-pTC5	121.2	120.6	118.1	110.6	111.0[c]	109.7[c]	111.1	113.2	111.5
-pTC6	131.9	130.6	130.4	122.2	122.3	121.3	122.5	123.0	121.8
-pTCH_3	19.8	19.3	18.6	15.4	16.2	15.6	19.7	20.6	19.2
-pTC1′	87.9	88.2	86.3	85.1	86.6	84.4	85.5	86.6	84.7
-pTC2′	40.6	40.9	38.9	39.1	40.0	38.9[e]	36.5	37.4[c]	36.3[d]
-pTC3′	71.3	71.4	69.7	71.7	72.7	70.2	71.7	72.7	69.9[c]
-pTC4′	86.7[c]	86.4[c]	85.4[c]	85.2	85.4[d]	83.3	85.1	85.0[d]	83.2[e]
-pTC5′	65.9	66.6	64.8	65.2	68.5	64.1	65.9	68.8	65.3
N^3-CH_3	36.8	35.8	35.2	29.6	30.6	29.6[d]	35.6	36.7[c]	35.3[d]
p-CH_3		11.1	10.8		11.0	9.6		11.7	9.5

[a] Recorded in DMSO-d_6. [b–e] May be interchanged.

Table 4. Intensity[a] of NOEs Used in Conformational and Configurational Assignments of 12a–c and 13a–c in D_2O

	Tp-						-pT					
protons	**12a**	**12b**	**12c**	**13a**	**13b**	**13c**	**12a**	**12b**	**12c**	**13a**	**13b**	**13c**
Intranucleoside NOEs												
H6/H1′	a	w	w	s	s	s	a	a	a	w	w	w
H6/H2′	m	m	a	a	a	a	s	s	s	s	s	s
H6/H3′	s	s	s	a	a	a	s	s	s	s	s	s
H6/CH_3	s	s	s	s	s	s	s	s	s	s	s	s
Internucleoside NOEs												
Tp-H6/-pTCH_3	s	s	s	a	a	a						
Tp-H6/N^3-CH_3	a	a	a	s	s	s						
Tp-CH_3/-pTCH_3	s	s	s	a	a	a						
Tp-CH_3/N^3-CH_3	a	a	a	s	s	s						

[a] s: strong; m: medium; w: weak; a: absent.

Table 5. ^{1}H NMR Chemical Shift Data for 14a–c in D_2O

	Tp-			-pT		
proton	**14a**	**14b**	**14c**	**14a**	**14b**	**14c**
H1′	6.36	6.37	6.34	6.19	6.15	6.10
H2′	2.58	2.59	2.56	2.26	2.11	2.16
H2″	2.58	2.74	2.76	2.11	2.11	2.16
H3′	4.71	5.02	4.72	4.59	4.49	4.56
H4′	3.98	4.05	4.07	3.98	4.05	3.91
H5′	3.84	3.81	3.76	3.98	4.23	4.27
H5″	3.98	3.98	4.01	3.98	4.23	4.27
H7 *pro-R*	2.58	2.55	2.49			
H7 *pro-S*	3.20	3.18	3.17			
CH_3				1.97	1.93	1.88
N^3-CH_3				2.94	2.93	2.93
H6	7.27	7.35	7.34	6.68	6.52	6.29
p-CH_3		1.72	1.83			

Compounds **12b** and **12c** arose by cycloaddition between the two pyrimidine bases in anti glycosyl conformation as in the case of **12a**.

The ^{1}H NMR spectra of **13b** and **13c** (Table 2) were similar to the spectrum of known **13a**[9a] as were the corresponding 2D phase-sensitive NOESY data (Table 4) establishing that **13b** and **13c** were the methylphosphonate analogs of **13a**. Thus, the configurations at C5 and C6 of the 5′-base were both *S* and the one at C4 of the 3′-base was *S*.

Photoproducts 14a–c. The UV spectrum of **14a–c** displayed a maximum at 267 nm indicating the absence of the thiocarbonyl chromophore. Comparison of the ^{1}H and ^{13}C NMR data of **14a–c** (Tables 3 and 5)[17] with those of their respective starting materials *i.e.*, **1b, 11a–b** (Tables 3 and 6),[18] revealed the absence of Tp-C5 methyl group and the presence of a methylene system (δ_H: 2.5 and 3.2 ppm; δ_C: *ca.* 30 ppm). Coupling of the latter

(17) Complete ^{1}H and ^{13}C NMR spectral assignments of **14a** were performed by ^{13}C–^{1}H COSY and long range ^{13}C–^{1}H COSY experiments. Quaternary carbons were identified from the following sets of long range carbon–proton correlations: C2 and C4 carbons correlated with H6 proton of their own base (^3J); -pT C2 – N^3-methyl protons (^3J); -pTCH_3 – -pTC4 (^3J); -pTC5 – -pT methyl proton (^2J) and Tp-C5 – CH_2 7 protons (^2J). The assignment of ^{1}H and ^{13}C NMR resonances of **14b-c** were made first by comparison with those of **14a** then further confirmed (except quaternary carbons) by HMQC experiment for **14b** and ^{13}C–^{1}H COSY experiment for **14c**.

Table 6. ^{1}H NMR Chemical Shift Data for 1b and 11a–b in D_2O[a]

	Tp-			-pT		
proton	**1b**[10]	**11a**	**11b**	**1b**[10]	**11a**	**11b**
H1′	6.12	6.15	6.16	6.29	6.26	6.26
H2′	2.29	2.42	2.44	2.43	2.42	2.44
H2″	2.52	2.42	2.44	2.43	2.42	2.44
H3′	4.80	5.05	5.06	4.59	4.52	4.56
H4′	4.17	4.20	4.22	4.17	4.20	4.22
H5′	3.78	3.76	3.74	4.09	4.36	4.34
H5″	3.78	3.76	3.74	4.17	4.36	4.34
CH_3	1.85	1.76	1.89	2.10	2.08	2.13
N^3-CH_3				3.69	3.69	3.71
H6	7.63	7.63	7.60	7.74	7.61	7.63
p-CH_3		1.72	1.73			

[a] A minimum amount of DMSO-d_6 was added to provide solubility in D_2O.

protons with C5 of the Tp- base on the long range ^{13}C–^{1}H COSY spectrum of **14a** indicated that this methylene carbon was attached to carbon C5 of the Tp- base. The absence of the -pTC4 thiocarbonyl function was confirmed by the lack of ^{13}C resonance near 190 ppm. Instead, a quaternary sp^3 carbon signal (δ_C: 90 ppm) was assigned to the C4 carbon of the -pT base from its long range coupling with both -pTH6 proton and -pT methyl protons (^3J) on the long range ^{13}C–^{1}H COSY spectrum. The sp^3 hybridization of this carbon was further confirmed by the shielding of both the -pTH6 proton ($\Delta\delta_H$: 1.1–1.3 ppm) and C6 carbon ($\Delta\delta_C$: 8–10 ppm) together with N^3-methyl protons ($\Delta\delta_H$: 0.75–0.78 ppm) and N^3-methyl carbon ($\Delta\delta_C$: 5–7 ppm) located in the β position and the shielding of the vicinal -pTC5 carbon ($\Delta\delta_C$: 8–11 ppm) compared to the corresponding signals in **1a** and **11a–b**.

No molecular ion could be detected by FABMS for these three compounds. However, in electrospray mode, $(M + H)^+$ ions were observed at *m/z* 561 for **14a** and *m/z* 559 for **14b–c**, *i.e.*, 16 amu less than for their respective starting materials **1b** and **11a–b**.

All these structural informations were consistent with the presence of both a methylene carbon bridging Tp-C5 and -pTC4 carbons and a quaternary sp^3 at the -pTC4 carbon bearing a hydroxyl group. Thus, photoproducts **14a–c** resulted from a combination of a methylene radical generated from the methyl of the 5′-base with a C4 centered radical of the 3′-base, the initially formed thiol group being finally replaced by an hydroxyl group (Scheme 3).[9b] A similar photochemical pathway has been observed with a thiolated dimer analog having a reverse sequence.[19]

The 2D phase sensitive NOESY data of **14a–c** (Table 7) established an anti glycosyl orientation of both bases indicating that these compounds resulted from photochemical reactions of an intermediate having the bases in the same anti glycosyl conformation. As expected for such base orientations, Tp-H6 proton gave NOEs with both -pT methyl protons and -pTH6 proton. The *R* configuration at -pTC4 was governed by geometric factors which prevented an attack of the methylene radical on the *Re* face of the thio-substituted C4-radical, the 3′-base being anti oriented.

(18) The assignment of proton and protonated carbon signals of **1b**, **11a,b** were performed with ^{13}C–^{1}H COSY experiments. Quaternary carbons of **1b** were assigned from long range ^{13}C–^{1}H COSY experiment.

(19) Fourrey, J.-L.; Gasche, J.; Fontaine, C.; Guittet, E.; Favre, A. *J. Chem. Soc., Chem. Commun.* **1989**, 1334–1336.

Table 7. Intensity[a] of NOEs Used in Conformational and Configurational Assignments of 14a–c and 15a–b in D_2O

	Tp-					-pT				
protons	**14a**	**14b**	**14c**	**15a**	**15b**	**14a**	**14b**	**14c**	**15a**	**15b**
Intranucleoside NOEs										
H6/H1′	w	w	w	o	s	w	w	w	*b*	a
H6/H2′	a	a	a	s	o	s	s	s	s	s
H6/H3′	s	s	s	m	b	s	s	s	s	s
H6/H7 *pro-R*	s	s	s	s	a					
H6/H7 *pro-S*	a	a	a	a	s					
Internucleoside NOEs										
Tp-H6/-pTH6	m	m	m	o	a					
Tp-H6/-pTCH_3	s	s	s	s	o					
Tp-H6/N^3-CH_3	a	a	a	a	s					
H7 *pro-R*/-pTCH_3	s	s	s	s	a					
H7 *pro-S*/N^3-CH_3	s	s	s	m	s					

[a] s: strong; m: medium; w: weak; a: absent; o: overlap. [b] Signals are too close to evaluate the off-diagonal peak.

Table 8. ^{1}H NMR Chemical Shift Data for 15a and 15b in D_2O (a) and DMSO-d_6 (b)

	Tp-				-pT			
proton	**15a** (a)	**15a** (b)	**15b** (a)	**15b** (b)	**15a** (a)	**15a** (b)	**15b** (a)	**15b** (b)
H1′	6.25	6.22	5.30	5.33	6.25	6.30	6.10	6.18
H2′	2.18	2.13	2.38	2.10	2.36	2.32	2.38	2.39
H2″	2.60	2.51	2.93	2.82	2.18	1.98	2.22	2.10
H3′	4.98	4.99	*a*	4.87	4.50	4.24	4.37	4.00
H4′	3.83	4.18	4.50	3.93	3.75	3.92	3.72	4.01
H5′	3.69	*b*	3.74	3.58	4.19	4.13	4.11	3.93
H5″	3.69	*b*	3.74	3.58	4.30	4.13	4.29	4.23
H6	4.54	4.51	4.89	5.00	6.25	6.33	6.35	6.40
CH_3					1.96	2.06	1.73	1.80
H7 *pro-R*	3.28	3.14	3.62	3.65				
H7 *pro-S*	3.60	*b*	3.39	3.36				
N^3-CH_3					3.04	2.94	3.16	3.18
p-CH_3					1.67	1.59	1.70	
H5 Tp-	*c*	*b*	*c*	3.78				

[a] Obscured by HDO peak (4.8 ppm). [b] Under H_2O peak (around 3.5 ppm), this peak was shifted out of this region by acquiring that data at 50 °C, in this case Tp-H5′ and H5″ resonated at 3.59 and 3.70 ppm, *pro-S* H7 at 3.65 ppm, and H5 at 3.47 ppm. [c] Exchanged.

Assignment of the *pro-R* H7 proton of **14a–c** was deduced from its NOEs with the Tp-H6 proton and -pT methyl protons since they were located on the same side of the methylene bridge. As expected, the *pro-S* H7 proton gave a NOE with the N^3-methyl protons.

Photoproducts 15a–b. The ^{1}H NMR spectrum of **15a** and **15b** showed instead of Tp– methyl resonances two signals at 3.3 and 3.6 ppm (Table 8) suggesting the presence in **15a–b** of a methylene carbon located at the C5 position of the 5′-base. The shielding of the Tp-H6 proton signal ($\Delta\delta$: 2.4 and 2.8 ppm), compared to the corresponding signal in **14b** and **14c** indicated saturation of the C5–C6 double bond of the 5′-base. The absence of thiocarbonyl function was deduced from the UV spectrum (λ_{max} 250 nm and no absorption above 280 nm). The molecular formula of **15b**, established as $C_{22}H_{31}N_4O_{10}$-PS by HRFABMS, indicated that these photoproducts had the same molecular composition as their starting material **11a–b**. At this stage, two structures **15** and **16** could be proposed to fit the UV and MS data as well as the structural information gathered from the ^{1}H NMR spectra. Structure **16** was ruled out on the basis of mechanistic considerations (Scheme 3). In these compounds, as it will be shown below, the -pT base has been found to be anti oriented; thus, they must have derived from a biradical precursor exhibiting the same 3′-end *N*-glycosidic conformation. Accordingly, **16** should have

resulted from a radical coupling taking place between the methylene radical approaching the *Re* face of the thiol-substituted C4-radical with the last step being the Michael addition of the thiol to the C5–C6 double bond of T*p*-. However, such an attack must be precluded for geometric factors in the case of an anti-oriented 3′-base. Conversely, structure **15** arose from radical coupling between the T*p*-C6 radical approaching the *Si* face of the -*p*TC4 radical which is readily accessible when the 3′-base is anti oriented, thus fixing the *S* configuration at -*p*TC4. The radical coupling step was followed by the Michael addition between the thiol group and the exo methylene function of the intermediate.

Due to keto–enol equilibrium which may occur within 5,6-dihydro pyrimidinone, it was anticipated that T*p*-H5 might undergo exchange during NMR measurement in D_2O.[6a,c,e,20] Indeed, when recorded in D_2O, the ^1H NMR spectra of **15a** and **15b** displayed a singlet for the H6 proton of the 5′-base and were devoid of the signal due to T*p*-H5. This H5 proton signal could be observed when the ^1H NMR spectrum was recorded in DMSO-d_6. Moreover, the T*p*-H6 proton appeared as a doublet and the shielded H7 proton signal showed an additional coupling, consistent with the vicinal coupling between these protons and H5.

The ^{13}C NMR spectrum of **15b** (D_2O) further confirmed saturation of the T*p*- C5–C6 bond and the presence of a -*p*TC4 sp^3 carbon. It showed a signal at 68 ppm attributed to the T*p*- C6 carbon on the basis of its scalar coupling with the T*p*-H6 proton signal at 4.89 ppm on the ^{13}C–^1H COSY spectrum. This assignment was further substantiated by a long range coupling observed between T*p*-H6 and T*p*-C4 and T*p*-C2 (^3J) carbons on the HMBC spectrum. A carbon resonance at 87 ppm, assigned to -*p*TC4 carbon from its scalar long range coupling with the -*p*T methyl, N^3 methyl and -*p*TH6 protons (^3J), was also observed. Additional carbon signals at 31 ppm corresponding to the methylene carbon and that of a very small T*p*-C5 sp^3 signal at 48 ppm due to deuterium substitution were also detected. The HMBC spectrum showed a correlation between the -*p*TC4 carbon and both T*p*-H6 and the deshielded H7 protons.

Stereochemistry at the C5 and C6 carbons of **15a–b** was deduced from the NMR data. In the case of (*Sp*)-**15b**, the 2D phase sensitive NOESY data recorded in D_2O (Table 7) established the syn and anti orientations for the 5′-base and the 3′-base, respectively. As expected for such orientations, T*p*- H6 proton gave a NOE with N^3-methyl protons since they were located on the same side of the tetrahydrothiophene ring. The syn orientation of the 5′-base implied a *S* configuration at C6. The T*p*-H6 proton gave a strong correlation on the 2D phase sensitive NOESY spectrum recorded in DMSO-d_6 with the T*p*-H5 proton indicating that these two protons were located on the same side of the plane of the dihydropyrimidine ring. Thus, C5 was found to be *S*, and it was concluded that substituents at C5 and C6 were cis. From X-ray and NMR studies, 5,6-dihydrothymines were found to adopt half-chair conformations.[6a] The coupling constant between T*p*-H5 and T*p*-H6 protons, thus in a pseudoaxial–pseudoequatorial relationship, was 8 Hz in accordance with literature data.[6e] For the 5′-base of **15b**, two half-chair conformations could be considered: one with carbon C5 below and carbon C6 above the plane of the other four atoms with subsituents at C5 pseudoequatorial and C6 pseudoaxial and *vice versa*. In compound **15b** the *pro-S* H7 proton was assigned from its NOE with the T*p*-H6 proton and N^3-methyl protons. The absence of vicinal coupling between the T*p*-H5 proton and the *pro-R* H7 proton indicated an orthogonal spatial arrangement of these protons. Such a spatial arrangement could only fit with an half-chair conformation of the dihydropyrimidine with C5 below and C6 above the plane of the other four atoms. In the case of (*Rp*)-**15a**, the anti glycosyl conformation of the two bases was defined by a phase sensitive NOESY spectrum recorded in D_2O (Table 7). The anti orientation of the 5′-base implied a C6 *R* configuration. As the magnitude of the coupling constant (8 Hz) between T*p*-H5 and T*p*-H6 protons was the same as in **15b**, we deduced that these protons were also in a pseudoaxial–pseudoequatorial orientation, *i.e.*, in a cis relationship; thus the configuration at carbon C5 was *R*. Confirmation of the cis relationship of these protons was brought by a 1D-NOE experiment recorded in DMSO-d_6 at 50 °C to shift out the H_2O signal from the T*p*-H5 region. Irradiation of the T*p*-H6 proton gave an enhancement of the T*p*-H5 signal. The *pro-R* H7 proton was assigned from its NOE with T*p*-H6 proton and -*p*T methyl protons. The *pro-S* H7 proton gave, as expected, a NOE with N^3-methyl protons. The absence of a vicinal coupling between T*p*- H5 and the *pro-S* H7 proton was indicative of an orthogonal spatial arrangement. Such a spatial arrangement could only fit with a half-chair conformation of the dihydropyrimidine with C5 above and C6 below the plane of the other four atoms. The T*p*- H1′ proton of **15b** was shielded ($\Delta\delta$: 0.9 ppm) compared to the one of **15a** due to the syn orientation of the 5′-end *N*-glycosidic bond; a same trend was observed within the thietane series going on from the anti to syn orientation of the 5′-end *N*-glycosidic bond.

Derivatives 17 and 18. Compounds **17** and **18** were both isolated during the desalting step of a collected peak (retention time 13.8 mn) which showed UV absorption maxima at 267 and 319 nm. These two compounds apparently resulted from a complicated series of reactions which involved hydrolysis of the 3′-end *N*-glycosidic bond of photoproduct **14c** with rearomatization of the 3′-base, loss of the 3′-end deoxyribose, and additional loss of the phosphorus atom in the case of **17**.

The presence of a methylene carbon bridging the C5 carbon of the 5′-base to the C4 carbon of the 3′-base in **17** and **18** was deduced, as for the photoproducts **14a–c**, from (i) the absence of any T*p*- methyl proton signals on the ^1H NMR spectrum of **17** and **18**, (ii) lack of the corresponding carbon signal on the ^{13}C NMR spectrum of **17**, (iii) the presence of two methylene protons resonating at 3.87 ppm for **17** and 3.85 ppm for **18**, and (iv) the presence of a signal at 28.6 ppm in the ^{13}C NMR spectrum of **17**.

The UV spectrum of these two compounds, displaying maxima at 267 and 317 nm, indicated that the 3′-base was rearomatized. This was further confirmed by the deshielding of -*p*T H6 proton and -*p*TC6 carbon resonances ($\Delta\delta_H$: *ca.* 1.9 ppm and $\Delta\delta_C$: *ca.* 47 ppm) compared to the corresponding signals in compounds **14a–c**.

The elimination of the -*p*T deoxyribose in **17** and **18** was easily detected by the absence of the corresponding signals on the ^1H and ^{13}C NMR spectra. The methylphosphonate monoester in compound **18** was characterized by the presence of shielded *P*-methyl protons in the ^1H NMR spectrum (δ_H: 1.27 ppm, d, J = 16.2 Hz)

(20) Clivio, P.; Favre, A.; Fontaine, C.; Fourrey, J.-L.; Gasche, J.; Guittet, E.; Laugâa, P. *Tetrahedron* **1992**, *48*, 1605–1616.

compared to the one of **14a** and the chemical shift value of a phosphorus signal in the ^{31}P NMR spectrum (26.76 ppm).[21] The FABMS of **17** and **18** (see Experimental Section) were in full agreement with the proposed structures.

Photoproduct 19. The FABMS spectrum of compound **19** displayed an ion at *m/z* 559 $(M + H)^+$ (*i.e.*, 16 amu less than for its starting material **11b**), and its UV spectrum indicated lack of the thiocarbonyl (265 nm). Since the only significant difference between the ^1H NMR spectra of **19** and **11b** was the shielding of the N^3-methyl group ($\Delta\delta$: 0.42 ppm), we concluded that **19** was most likely the desulfurized analog of **11b**.

Photoproduct 20. The UV spectrum of **20** (λ_{max} 264 nm) revealed the absence of thiocarbonyl function. Compared to **11b**, the ^1H NMR spectrum of **20** lacked the T*p*-methyl signal and showed a singlet due to two protons resonating at 4.32 ppm. Further confirmation of the presence of a methylene carbon attached to C5 of the T*p*-base was brought by the NOESY spectrum which showed correlation between T*p*- H6 proton and the methylene protons at 4.32 ppm. The FABMS of **20** displayed an ion at *m/z* 597 $(M + Na)^+$ suggesting the same molecular weight as **11b**. From these structural elements, it was evident that the thiocarbonyl had been replaced by a carbonyl group and the T*p*- methyl group by a hydroxymethyl group. As for compound **19**, in comparison to **11b**, replacement of the thiocarbonyl by a carbonyl function in **20** induced a shielding of 0.47 ppm of the N^3-methyl proton signal.

Conclusion

The comparison of the photoreactivity of N^3-methyl-4-thiothymine containing dinucleoside phosphate **1b** with that of its methylphosphonate analogs (*Rp*)-**11a** and (*Sp*)-**11b** has shown that the three dimers exhibit a very similar behavior which can be rationalized on the basis of a common photochemical mechanism. However, some significant differences could be noticed concerning the kinetics of the photoreactions and the nature and stability of the photoproducts. The rate of photolysis for each dimer decreased in the order **1b** > **11a** > **11b**. This means that the conformational mobility, which permits the two pyrimidine residues to come in a close proximity at a bonding distance and to adopt a suitable relative orientation was, to some extent, affected by the modification of the phosphate–sugar backbone and, also, by the absolute configuration at the phosphorus center. Under the experimental conditions investigated the methylphosphonate with the *Rp* configuration was found to be a better mimic, as judged from its photochemical behavior, of the natural internucleotidic bond than its *Sp* diastereomer. Moreover, this study on dinucleoside methylphosphonate analogs led to the discovery of a new type of photoproduct corresponding to **15**. It can be surmised that similar compounds might also be formed in irradiated DNA; however, due to isolation problems, they might have been overlooked.

Experimental Section

Synthesis. Pyridine was dried by refluxing with CaH_2 overnight followed by distillation and redistillation from *p*-toluenesulfonyl chloride and stored over 4 Å molecular sieves. Acetonitrile was dried by refluxing with CaH_2 overnight followed by distillation and stored over 4 Å molecular sieves. Dioxane was dried by distillation from $LiAlH_4$ and storage over Na-wire. Tetrahydrofuran was dried by distillation from $LiAlH_4$ directly before use. Chloroform was passed through basic Al_2O_3 prior to use. Triethylammonium bicarbonate buffer was prepared by passing CO_2 gas through a mixture of triethylamine and water until saturation. The Lawesson reagent, *tert*-butyldiphenylsilyl chloride, imidazole, and tetrabutylammonium fluoride trihydrate were purchased from Aldrich and used without further purification. Thymidine and 4-methoxypyridine 1-oxide were purchased from Aldrich and dried over P_2O_5 overnight at 70 °C and 0.2 mmHg. Methylphosphonic dichloride,[22] 2-chloro-5,5-dimethyl-2-oxo-1,3,2-dioxaphosphinane,[23] and N^3-methylthymidine[24] (**2**) were prepared according to the published procedures. For all column purifications, silica gel, 230–400 mesh, purchased from Amicon Europe was used, and the columns were run in flash mode. Reported yields are referring to products obtained after drying at $p < 1$ mmHg for at least 24 h.

^1H, ^{13}C, and ^{31}P NMR spectra were recorded on a JEOL GSX-270 FT spectrometer. ^1H NMR chemical shifts are given in ppm relative to tetramethylsilane in $CDCl_3$ (25 °C) or sodium 3-(trimethylsilyl)propionate-2,2,3,3-d_4 in DMSO-d_6 (50 °C), ^{13}C chemical shifts recorded in $CDCl_3$ (25 °C) or DMSO-d_6 (50 °C) are given using the corresponding residual solvent signals as references ($CDCl_3$: 77.17 ppm; DMSO-d_6: 41.20 ppm); ^{31}P chemical shifts are reported to an external reference (2% H_3PO_4 in H_2O) in $CDCl_3$ (25 °C) or DMSO-d_6 (50 °C). *J* values are given in Hz.

Mass spectra were recorded in a JEOL MS SX 102 spectrometer with *m*-nitrobenzyl alcohol as a matrix and with sodium acetate as a source of sodium ions.

3′,5′-Di-*O*-benzoyl-N^3-methylthymidine (3). N^3-Methylthymidine[24] (**2**), (6.33 g, 24.7 mmol) was dried by evaporation of added pyridine and dissolved in the same solvent (200 mL). The reaction mixture was cooled with an ice bath, and benzoyl chloride (7.2 mL, 62 mmol) was added in 10 portions during 2 min. The cooling bath was removed and the reaction mixture stirred at ambient temperature for 1 h. The mixture was cooled again, and water (10 mL) was added to decompose excess benzoyl chloride. After evaporation to near dryness, the residue was partitioned between $CHCl_3$ (200 mL) and saturated aqueous $NaHCO_3$ (200 mL). The organic phase was dried over Na_2SO_4 and evaporated to give chromatographically homogeneous **3** (11.36 g, 99%) as a white solid: ^1H NMR ($CDCl_3$) 1.66 (3 H, d, J = 1.1), 2.34 (1 H, m), 2.72 (1 H, ddd, J = 14.3, 5.5, 1.5), 3.34 (3 H, s), 4.54 (1 H, m), 4.68 (1 H, dd, J = 12.1, 3.5), 4.81 (1 H, dd, J = 12.1, 2.9), 5.66 (1 H, m), 6.50 (1 H, dd, J = 8.8, 5.5), 7.26 (1 H, s), and 7.44–8.08 (10 H, m); ^{13}C NMR ($CDCl_3$) 13.0, 28.0, 38.2, 64.4, 75.1, 82.7, 85.8, 110.8, 128.7, 128.9, 129.1, 129.4, 129.6, 129.9, 132.3, 133.8, 133.8, 151.1, 163.5, and 166.1.

N^3-Methyl-4-thiothymidine[9] (4). 3′,5′-Di-*O*-benzoyl-N^3-methylthymidine (**3**) (9.29 g, 20.0 mmol) was dried by evaporation of added pyridine and dissolved in dioxane (200 mL). The Lawesson reagent (8.09 g, 20.0 mmol) was added and the reaction mixture stirred under reflux with exclusion of moisture. After 2 h when TLC showed the presence of unreacted **3**, another portion of the Lawesson reagent (8.09 g, 20.0 mmol) was added. The reaction mixture was refluxed for another 16 h, heating was discontinued, and the reaction mixture was cooled on an ice bath. Water (20 mL) was added and the mixture stirred for 1 h. The reaction mixture was concentrated to a yellow oil which was partitioned between $CHCl_3$ (400 mL) and saturated aqueous $NaHCO_3$ (400 mL). Drying over Na_2SO_4 and evaporation of the organic phase gave crude 3′,5′-dibenzoyl-N^3-methyl-4-thiothymidine as a yellow foam. Debenzoylation was performed in 50 mM NaOMe/MeOH solution (200 mL) under reflux for 30 min. Crude **4** was obtained as a

(21) Freeman, S.; Irwin, W. J.; Mitchell, A. G.; Nicholls, D.; Thomson, W. *J. Chem. Soc., Chem. Commun.* **1991**, 875–877.

(22) Agarwal, K. L.; Riftina, F. *Nulceic Acids Res.* **1979**, *6*, 3009–3024.

(23) Stec, W.; Zwierzak, A. *Can. J. Chem.* **1967**, *45*, 2513–2520.

(24) Tanabe, T.; Yamauchi, K.; Kinoshita, M. *Bull. Chem. Soc. Jpn* **1979**, *52*, 204–207.

yellow oil after cooling, neutralization (Dowex 50W H^+-form), and evaporation of the solvent. Column chromatography of this material using a stepwise gradient of MeOH (0–10%) in $CHCl_3$ as eluent afforded homogeneous **4** (2.26 g, 41%) as yellow crystals.

5′-*O*-(Dimethoxytrityl)-N^3-methyl-4-thiothymidine (5). N^3-Methyl-4-thiothymidine (**4**) (0.68 g, 2.50 mmol) was dried by evaporation of added pyridine and dissolved in the same solvent (12.5 mL). Triethylamine (0.42 mL, 3.0 mmol) was added and the reaction mixture cooled on an ice bath. Dimethoxytrityl chloride (0.93 g, 2.7 mmol) was added, the cooling bath removed, and the reaction mixture stirred at ambient temperature for 16 h. Partitioning of the reaction mixture between $CHCl_3$ (2 × 25 mL) and saturated aqueous $NaHCO_3$ (50 mL) followed by drying over Na_2SO_4 and evaporation of the organic phase gave crude **5** as a yellow foam. Traces of pyridine were removed by evaporation of added acetonitrile. Column chromatography using a stepwise gradient of MeOH (0–3%) in $CHCl_3$:Et_3N (995:5) as eluent afforded **5** (1.18 g, 82%) as a yellow foam: ^1H NMR ($CDCl_3$) 1.75 (3 H, s), 2.32 (1 H, m), 2.50 (1 H, m), 3.38 (1 H, dd, J = 10.4, 2.9), 3.51 (1 H, dd, J = 10.4, 3.3), 3.79 (6 H, s), 3.80 (3 H, s), 4.08 (1 H, m), 4.55 (1 H, m), 6.36 (1 H, pst, J = 6.4), 6.83 (4 H, d, J = 8.4), 7.23–7.41 (9 H, m), and 7.65 (1 H, s); ^{13}C NMR ($CDCl_3$) 18.8, 35.7, 41.5, 55.4, 63.4, 72.1, 86.4, 86.5, 87.1, 113.9, 120.0, 127.3, 128.1, 128.2, 128.9, 130.2, 135.5, 144.4, 149.2, 158.8, and 191.4.

3′-*O*-(*tert*-Butyldiphenylsilyl)-N^3-methyl-4-thiothymidine (6). 5′-*O*-(Dimethoxytrityl)-N^3-methyl-4-thiothymidine (**5**) (1.15 g, 2.00 mmol) was dried by evaporation of added pyridine and dissolved in DMF (10 mL). Imidazole (0.48 g, 6.0 mmol) was added, followed by TBDPS-Cl (0.78 mL, 3.0 mmol). The reaction mixture was stirred at room temperature until TLC indicated complete reaction (ca. 3 h). The reaction mixture was transferred to a separatory funnel and diluted with toluene (50 mL) and the DMF removed by extraction with water (3 × 50 mL). Drying over Na_2SO_4 and evaporation of the organic phase gave a yellow foam which was dissolved in $CHCl_3$:MeOH (7:3, 40 mL). After the mixture was cooled on an ice bath, $TsOH{\cdot}H_2O$ (2.0 g, 11 mmol), was added. The cooling bath was removed and the reaction mixture stirred at ambient temperature for 20 min. Standard workup followed by column chromatography using toluene:ethyl acetate (9:1) as eluent afforded **6** (806 mg, 79%) as a yellow foam: ^1H NMR ($CDCl_3$) 1.09 (9 H, s), 2.09 (3 H, s), 2.19 (1 H, m), 2.40 (1 H, m), 3.27 (1 H, dd, J = 11.7, 2.9), 3.66 (1 H, J = 12.1, 2.6), 3.78 (3 H, s), 4.00 (1 H, m), 4.45 (1 H, m), 6.22 (1 H, pst, J = 6.6), and 7.37 (11 H, m); ^{13}C NMR ($CDCl_3$) 19.1, 19.3, 27.0, 35.6, 40.8, 62.0, 72.7, 88.0, 88.3, 119.7, 128.1, 130.0, 133.1, 133.3, 135.8, 135.9, 149.1, and 191.3.

5′-*O*-(*tert*-Butyldiphenylsilyl)thymidine (8). Thymidine (**7**) (4.84 g, 20.0 mmol) was suspended in DMF (20 mL). Imidazole (3.00 g, 44.0 mmol) was added followed by TBDPS-Cl (5.72 mL, 22.0 mmol). The reaction mixture was stirred at room temperature until TLC indicated complete reaction (~2 h). The reaction mixture was evaporated (p ~ 1 mmHg) to near dryness. Column chromatography of the residue using a stepwise gradient of MeOH (0–6%) in $CHCl_3$ gave **8** (7.13 g, 74%) as a white foam: ^1H NMR was in accordance with published data;[11] ^{13}C NMR ($CDCl_3$) 12.1, 19.4, 27.0, 41.1, 64.3, 72.2, 84.9, 87.4, 111.3, 128.0, 130.1, 130.2, 132.4, 133.0, 135.3, 135.6, 150.9, and 164.3.

5′-*O*-(*tert*-Butyldiphenylsilyl)thymidine 3′-(Methylphosphonate) Triethylammonium Salt (9). Methylphosphonic dichloride[22] (liquified by gentle heating, 1.85 mL, 20.0 mmol) was dissolved in acetonitrile (100 mL), and imidazole (6.81 g, 100 mmol) was added. Voluminous precipitation of imidazolinium hydrochloride occurred immediately. After the mixture was stirred for 15 min at room temperature, 5′-*O*-(*tert*-butyldiphenylsilyl)thymidine (**8**) (4.81 g, 10.0 mmol, dried by evaporation of added pyridine and dissolved in pyridine, 20 mL) was added in one portion. The reaction mixture was stirred at room temperature until TLC showed complete disappearance of the starting material (ca. 5 h). TEAB-buffer (2 M, 20 mL) was added and the reaction mixture stirred for 5 min and concentrated. The oily residue was dissolved in $CHCl_3$ (100 mL) and washed with 1 M TEAB-buffer (200 mL). Extraction of the aqueous phase with $CHCl_3$ (100 mL) and evaporation of the combined organic layers gave crude **9** as a white foam. Column chromatography using a stepwise gradient of MeOH (0–20%) in $CHCl_3$:Et_3N (995:5) as eluent afforded **9** (6.09 g, 92%) as a white foam: ^1H NMR ($CDCl_3$) 1.09 (9 H, s), 1.24–1.32 (12 H, m), 1.52 (3 H, s), 2.22 (1 H, m), 2.57 (1 H, m), 2.95 (6 H, q, J = 7.3), 3.95 (2 H, m), 4.23 (1 H, m), 4.94 (1 H, m), 6.42 (1 H, dd, J = 8.8, 5.1), and 7.35–7.69 (11 H, m); ^{13}C NMR ($CDCl_3$) 8.9, 11.6, 12.3, 14.3, 19.4, 27.0, 40.0, 45.3, 64.2, 74.0, 74.1, 84.4, 86.3, 86.4, 111.1, 127.9, 127.9, 129.9, 130.0, 132.4, 133.1, 135.3, 135.6, 150.8, and 164.3; ^{31}P NMR ($CDCl_3$) 22.45.

5′-*O*-(*tert*-Butyldiphenylsilyl)thymidylyl-(3′ → 5′)-3′-*O*-(*tert*-butyldiphenylsilyl)-N^3-methyl-4-thiothymidine 3′-(Methylphosphonate) (10). 3′-*O*-(*tert*-Butyldiphenylsilyl)-N^3-methyl-4-thiothymidine (**6**) (0.77 g, 1.5 mmol), 5′-*O*-(*tert*-butyldiphenylsilyl)thymidine 3′-(methylphosphonate)triethylammonium salt (**9**) (1.65 g, 2.50 mmol), and 4-methoxypyridine 1-oxide (0.94 g, 7.5 mmol) were dried by evaporation of added pyridine and dissolved in the same solvent (30 mL). 2-Chloro-5,5-dimethyl-2-oxo-1,3,2-dioxaphosphinane[22] (1.38 g, 7.50 mmol) was added and the reaction mixture stirred at room temperature until TLC indicated complete condensation (~1 h). The reaction mixture was concentrated by evaporation, and the residue was partitioned between $CHCl_3$ (2 × 50 mL) and 1 M TEAB-buffer (100 mL). The combined organic layers were dried over Na_2SO_4 and evaporated to a yellow foam. Residual pyridine was removed by evaporation of added acetonitrile. Column chromatography using a stepwise gradient of MeOH (0–4%) in $CHCl_3$ afforded **10** as a diastereomeric mixture contaminated with a pyrophosphate byproduct derived from the coupling reagent. Separation of the diastereomers was achieved by HPLC (Dynamax silica column) using a linear gradient of ethyl acetate (50–100%) in toluene as eluent. The faster eluting isomer (R_p)-**10a** (520 mg, 33%) and the slower eluting isomer (S_p)-**10b** (599 mg, 38%) were obtained as yellow foams after evaporation of the appropriate fractions.

(R_p)-**10a**: ^1H NMR ($CDCl_3$) 1.07 (9 H, s), 1.09 (9 H, s), 1.34 (3 H, d, J = 17.6), 1.85 (1 H, m), 2.12 (3 H, s), 2.15 (1 H, m), 2.34 (1 H, m), 2.49 (1 H, m), 3.59 (1 H, m), 3.78 (3 H, s), 3.82 (1 H, dd, J = 11.7, 2.6), 4.11 (2 H, m), 4.33 (1 H, m), 5.11 (1 H, m), 6.30 (1 H, dd, J = 9.2, 5.1), 6.38 (1 H, dd, J = 7.7, 5.9), 7.35–7.66 (22 H, m), and 8.17 (1 H, br s); ^{13}C NMR ($CDCl_3$) 10.7, 12.1, 12.8, 19.1, 19.5, 26.9, 27.1, 35.6, 39.3, 41.2, 63.9, 64.7, 64.8, 73.1, 76.5, 76.6, 84.2, 85.6, 85.7, 85.8, 85.9, 86.9, 111.7, 120.0, 128.1, 128.2, 128.4, 130.3, 130.4, 132.0, 132.8, 133.1, 134.9, 135.3, 135.6, 135.8, 149.0, 150.4, 163.7, and 191.3; ^{31}P NMR ($CDCl_3$) 31.32.

(S_p)-**10b**: ^1H NMR ($CDCl_3$) 1.07 (9 H, s), 1.08 (9 H, s), 1.41, (3 H, d, J = 17.6), 1.56 (3 H, J = 1.1), 1.79 (1 H, m), 2.11 (3 H, s), 2.22 (1 H, m), 2.45 (2 H, m), 3.57 (1 H, m), 3.74 (2 H, m), 3.77 (3 H, s), 3.92 (1 H, dd, J = 11.4, 2.2), 4.06 (2 H, m), 4.21 (1 H, m), 5.11 (1 H, m), 6.35 (2 H, m), 7.32–7.66 (22 H, m), and 8.14 (1 H, br s); ^{13}C NMR ($CDCl_3$) 10.7, 12.1, 12.9, 19.2, 19.5, 26.9, 27.1, 35.6, 39.5, 39.6, 40.9, 63.9, 64.9, 65.0, 72.8, 76.3, 76.4, 84.4, 85.7, 85.8, 86.8, 111.7, 120.0, 128.1, 128.2, 128.3, 130.3, 132.1, 132.7, 132.9, 134.8, 135.3, 135.6, 135.7, 149.0, 150.5, 163.7, and 191.3; ^{31}P NMR ($CDCl_3$) 32.34.

Thymidylyl-(3′ → 5′)-methyl-4-thiothymidine 3′-(Methylphosphonate) (11). (R_p)-**10a** (315 mg, 0.3 mmol) or (S_p)-**10b** (315 mg, 0.3 mmol) was dissolved in THF (3 mL). Tetrabutylammonium fluoride trihydrate (6 mol/equiv) was added, and the reaction mixture was stirred at room temperature until TLC indicated complete desilylation (~3 h). The reaction mixture was passed through a short silica column, the solvent evaporated, and the residue purified by column chromatography using a stepwise gradient of MeOH (0–20%) in $CHCl_3$ affording (R_p)-**11a** (145 mg, 84%) and (S_p)-**11b** (128 mg, 74%) as yellow foams.

(R_p)-**11a**: UV (λ_{max} H_2O) 267, 330 nm; ^1H NMR (DMSO-d_6) 1.60 (3 H, d, J = 17.6), 1.82 (3 H, s), 2.13 (3 H, s), 2.29 (2 H, m), 2.36 (2 H, m), 3.65 (1 H, m), 3.71 (3 H, s), 4.07 (2 H, m), 4.15–4.35 (3 H, m), 5.06 (1 H, m), 6.23 (2 H, m), 7.69 (1 H, s), and 7.76 (1 H, s); ^1H NMR (300 MHz, D_2O) see Table 6; ^{13}C

NMR (DMSO-d_6) see Table 3; ^{31}P NMR (DMSO-d_6) 32.23; HRMS found M^+ 575.1560, $C_{22}H_{32}O_{10}N_4SP$ requires M 575.1577.

(S_p)-**11b**: UV (λ_{max} H_2O) 266, 329 nm; ^{1}H NMR (DMSO-d_6) 1.61 (3 H, d, J = 17.6), 1.83 (3 H, d, J = 1.1), 2.14 (3 H, d, J = 0.7), 2.29 (2 H, m), 2.38 (2 H, m), 3.66 (1 H, m), 3.71 (3 H, s), 4.07 (2 H, m), 4.23 (2 H, m), 4.32 (1 H, m), 5.05 (1 H, m), 6.23 (2 H, m), 7.70 (1 H, d, J = 1.1), and 7.75 (1 H, d, J = 0.7); ^{1}H NMR (300 MHz, D_2O) see Table 6; ^{13}C NMR (DMSO-d_6) see Table 3; ^{31}P NMR (DMSO-d_6) 32.40; HRMS found M^+ 575.1550, $C_{22}H_{32}O_{10}N_4SP$ requires M 575.1577.

Irradiation Conditions. All irradiation experiments were performed with a Hanau TQ 150 lamp (360 nm) at 0 °C in aqueous solutions (HPLC grade) under nitrogen.

Analytical Scale. Phosphonates **11a** and **11b** were dissolved in 30 μL of DMSO and diluted with water (2 mg/10 mL) and the solutions were irradiated for 8 hours. (At the suggestion of a reviewer phosphate **1a** was irradiated under the same indicated conditions in the presence and in the absence of DMSO. Both crude irradiation mixtures exhibited identical ^{1}H NMR spectra and analytical HPLC profiles ruling out a possible influence of DMSO on the reaction course.) Samples of 30 μL were withdrawn every 10 min and subjected to the HPLC analysis.

Preparative Scale. Aqueous solutions of phosphate **1a** (ammonium salt) (20–50 mg/100 mL) or phosphonates **11a** and **11b** (20 mg/100 mL, 300 μL DMSO was used for dissolution) were photolyzed until the ratio of the two maxima at 330 and 267 nm had reached 0.27 for phosphate **1a** and 0.6 for **11b** and 0.4 **11a**. The irradiated solutions were lyophilized to give residues which were purified by preparative HPLC.

Product Purification. Ammonium acetate was purchased from Fluka (ref 09689) and acetonitrile from BDH (ref UN 1648).

Analytical HPLC. Twenty μL of the irradiated solutions of **11a** and **11b** were injected onto a Nova-Pack C18 0.8 × 10 cm 6 μm column. A 20 min, 2 mL/min linear gradient of 10–30% acetonitrile in 0.05 M aqueous ammonium acetate (adjusted to pH 7 by addition of ammonia) followed by a 10 min plateau and then a 30 min linear gradient of 30–60% acetonitrile in 0.05 M aqueous ammonium acetate (pH 7), was used. A photodiode array detector (Waters 990) was employed.

Preparative HPLC. The irradiated samples of phosphate **1a** (10 mg/200 μL) were injected onto a 5 μm Nucleosil C18 reversed phase column (1 × 25 cm). The solvent system consisted of a 30 min (4 mL/min) linear gradient of 0–12% acetonitrile in 0.05 M aqueous ammonium acetate (pH 7), followed by 12% acetonitrile (isocratic mode) during 30 min. The effluent was monitored at 260 nm. Fractions were concentrated and desalted by filtration through a Lichroprep RP18 (60–63 μm) short column with water as eluent. The appropriate fractions were lyophilized to give residues which were stored at −18 °C.

The irradiated samples of methylphosphonates **11a–b** (10 mg/100 μL, H_2O, solubilized with a minimum amount of DMSO) were injected onto a Nova-Pack C18 2.5 × 10 cm, 6 μm Radial-Pack cartridge. The chromatographic system was the same as the one used for the analytical study. The flow rate was set at 19 mL/min. Fractions were concentrated and desalted by injection on the same column at a flow rate of 10 mL/min. The solvent consisted of water for 10 min, followed by a gradient of 0–25% acetonitrile for 10 min. The effluent was monitored at 260 nm.

Product Characterization. NMR Spectroscopy of Dinucleoside Phosphates and Methylphosphonates. ^{1}H NMR spectra were recorded on Bruker AC250, AM300, AC300-P, AM400, and AMX600 spectrometers. ^{13}C NMR spectra were recorded on Bruker AC 250 and AC 300-P spectrometers. ^{31}P NMR spectra were recorded on Bruker AC 300-P.

The samples were lyophilized twice in 99.8% D_2O and dissolved in 99.96% D_2O. ^{1}H chemical shifts (δ_H) are reported relative to residual HDO peak set at 4.8 ppm in deuterium oxide (D_2O) or to residual DMSO-d_5 set at 2.6 ppm. ^{13}C NMR chemical shifts (δ_C) are reported relative to an external capillary standard of dioxane (δ_C: 67.8 ppm). ^{31}P NMR chemical shifts (δ_P) are reported relative to an external capillary standard of 85% phosphoric acid.

2D phase-sensitive NOESY spectra[25] were recorded at 250 MHz using a 500 ms mixing time in all experiments. All observed NOEs were positive, corresponding to an extreme motional narrowing situation. Thus, this allowed us to rule out spin diffusion artifacts.[26] One-dimensional NOE experiments were run at 400 MHz (50 °C) with 1 s of irradiation time and a decoupling power of 30 dB. ^{13}C–^{1}H COSY and long range ^{13}C–^{1}H COSY experiments were performed at 62.5 or 75 MHz on Bruker AC250 or AC300-P and HMQC and HMBC experiments at 100 MHz on Bruker AM400 spectrometer using standard pulse sequences.

Assignments of the deoxyribose protons were performed from absolute value mode ^{1}H–^{1}H COSY spectra. Resonances of the 3′-end and 5′-end deoxyribose protons were differentiated from the multiplicity of either the H3′ signal of the 5′-end deoxyribose or the H5′H5″ signals of the 3′-end deoxyribose which are coupled to the phosphorus atoms. When these signals could not be located, this differentiation was achieved by the ^{13}C–^{1}H COSY spectrum: T*p*-H3′ or -*p*T H5′H5″ protons were easily recognized from their correlations with carbon doublets since the latter are coupled to the phosphorus atom. T*p*-H6 and -*p*TH6 protons were differentiated from NOESY spectra which displayed correlations with protons of their respective sugar.

The prochiral C2′ protons were assigned from observed NOE between H6 proton of the base and H3′ protons or H2′ (2′*R*) proton or between H1′ proton and H2″ (2′*S*) proton.

The prochiral C5′ protons were assigned pairwise to their specific residues.

Conformation about the *N*-glycosidic bond was determined from NOE correlations between the H6 base proton and the deoxyribose protons. Observation of an NOE between H6 proton and H1′ proton was characteristic of a syn orientation. Conversely, NOEs between H6 proton and H2′ or H3′ proton of its deoxyribose (depending on whether the deoxyribose ring adopt a C2′ endo or a C3′ endo conformation) was informative of an anti glycosyl conformation.

Mass Spectroscopy. Positive FABMS (thioglycerol/NaCl matrix) were recorded using a Kratos MS 80 mass spectrometer. HRFABMS were measured on an ZAB instrument, and electrospray mass spectra were recorded on a TRIO 2000VG spectrometer.

1b (Tpm^{3}s^{4}T): UV (λ_{max} H_2O) 267, 330 nm; ^{1}H NMR (400 MHz D_2O) see Table 6; ^{13}C NMR (62.5 MHz D_2O) see Table 3; ^{31}P NMR (D_2O) 0.40 ppm; FABMS *m/z* 577 $(M + H)^+$, 599 $(M + Na)^+$.

12a: UV (λ_{max} H_2O) 255 nm; ^{1}H NMR (400 MHz D_2O) see Table 2; ^{13}C NMR (62.5 MHz D_2O) see Table 3; ^{31}P NMR (D_2O) −0.520 ppm; FABMS *m/z* 599 $(M + Na)^+$, 577 $(M + H)^+$.

(*Rp*)-**12b**: UV (λ_{max} H_2O) 256 nm; ^{1}H NMR (300 MHz D_2O) see Table 2; ^{13}C NMR (75 MHz D_2O) see Table 3; ^{31}P NMR (D_2O) 36.22 ppm; FABMS *m/z* 597 $(M + Na)^+$.

(*Sp*)-**12c**: UV (λ_{max} H_2O) 254 nm; ^{1}H NMR (300 MHz D_2O) see Table 2; ^{13}C NMR (75 MHz D_2O) see Table 3; ^{31}P NMR (D_2O) 35.99 ppm; FABMS *m/z* 597 $(M + Na)^+$.

13a: UV (λ_{max} H_2O) sh 232 nm; ^{1}H NMR (400 MHz D_2O) see Table 2; ^{31}P NMR (D_2O) −0.103 ppm; FABMS *m/z* 599 $(M + Na)^+$.

(*Rp*) **13b**: UV (λ_{max} H_2O) 232 nm; ^{1}H NMR (250 MHz D_2O) see Table 2; ^{31}P NMR (D_2O) 35.95 ppm; FABMS *m/z* 597 $(M + Na)^+$.

(*Sp*) **13c**: UV (λ_{max} H_2O) 234 nm; ^{1}H NMR (300 MHz D_2O) see Table 2; ^{31}P NMR (D_2O) 35.23 ppm; FABMS *m/z* 597 $(M + Na)^+$.

14a: UV (λ_{max} H_2O) 267 nm; ^{1}H NMR (400 MHz D_2O) see Table 5; ^{13}C NMR (62.5 MHz D_2O) see Table 3; ^{31}P NMR (D_2O) −0.348 ppm; MS (electrospray) *m/z* 561.2 $(M + H)^+$; 583.0 $(M + Na)^+$; 543.2 $(M + H - H_2O)^+$.

(*Rp*)-**14b**: UV (λ_{max} H_2O) 267 nm; ^{1}H NMR (300 MHz D_2O) see Table 5; ^{13}C NMR (75 MHz D_2O) see Table 3; ^{31}P NMR

(25) Bodenhausen, G.; Kogler, H.; Ernst, R. R. *J. Magn. Res.* **1984**, *58*, 370–388.

(26) Wüthrich, K. *NMR of Proteins and Nucleic Acids*; Wiley-Interscience: New York, 1986.

(D_2O) 37.01 ppm; MS (electrospray) *m/z* 559.3 $(M + H)^+$, 541.1 $(M + H - H_2O)^+$.

(*Sp*)-**14c**: UV (λ_{max} H_2O) 266 nm; ^1H NMR (300 MHz D_2O) see Table 4; ^{13}C NMR (75 MHz D_2O) see Table 3; ^{31}P NMR (D_2O) 36.47 ppm; MS (electrospray) *m/z* 581.2 $(M + Na)^+$, 559.2 $(M + H)^+$, 541.2 $(M + H - H_2O)^+$.

(*Rp*)-**15a**: UV (λ_{max} H_2O) 249 nm; ^1H NMR (300 MHz D_2O, 400 MHz DMSO-d_6) see Table 8; ^{31}P NMR (D_2O) 36.02 ppm; MS (electrospray) *m/z* 597.4 $(M + Na)^+$.

(*Sp*)-**15b**: UV (λ_{max} H_2O) sh 250 nm; ^1H NMR (400 MHz D_2O, 600 MHz DMSO-d_6) see Table 6; ^{13}C (75 MHz D_2O) δ 9.9 (*p*-CH_3), 18.9 (-*p*TCH_3), 32.0 and 32.3 (CH_2 7 and N^3-CH_3), 36.4 and 38.7 (T*p*-C2′ and -*p*TC2′), 49.4 (T*p*-C5), 62.2 (T*p*-C5′), 66.5 (-*p*TC5′), 69.9 and 70.1 (T*p*-C6 and -*p*TC3′), 78.7 (T*p*-C3′), 82.8 (-*p*TC4′), 84.1 (-*p*TC1′), 85.2 (T*p*-C4′), 88.5 (-*p*TC4), 90.1 (T*p*-C1′), 107.0 (-*p*TC5), 123.8 (-*p*TC6), 153.1 and 153.8 (T*p*-C2 and -*p*TC2), 171.4 (T*p*-C4); ^{31}P NMR (D_2O) 35.72 ppm; FABMS *m/z* 597 $(M + Na)^+$; HRFABMS MH^+ 575.1546 ($C_{22}H_{32}N_4O_{10}SP$ requires 575.1577).

17: t_R 7.0 min; UV (λ_{max} H_2O) 267, 317 nm; ^1H NMR (300 MHz D_2O) 2.14 (3H, -*p*TCH_3), 2.17 (1H, T*p*-H2′*), 2.39 (IH, T*p*-H2″*), 3.55 (3H, N^3-CH_3), 3.57 (2H, T*p*-H5′; H5″), 3.87 (2H, CH_2 7), 4.0 (1H, T*p*-H4′), 4.32 (1H, T*p*-H3′), 6.25 (1H, T*p*-H1′), 7.42 (1H, T*p*-H6), 8.45 (1H, -*p*TH6); ^{13}C NMR (62.5 MHz D_2O) δ 14.8 (-*p*TCH_3), 28.6 (CH_2 7), 35.0 (N^3-CH_3), 40.7 (C2′), 62.3 (C5′), 72.0 (C3′), 87.0 (T*p*-C4′**), 88.5 (T*p*-C1′**), 109.7 (T*p*-C5), 117.9 (-*p*TC5), 138.6 (T*p*-C6), 167.5 (-*p*TC6); *Assigned only pairwise; **May be interchanged; FABMS *m/z* 387 $(M + Na)^+$, 365 $(M + H)^+$.

18: t_R 5.0 mn; UV (λ_{max} H_2O) 267, 317 nm; ^1H NMR (300 MHz D_2O) 1.27 (3H, *p*-CH_3), 2.13 (3H, -*p*TCH_3), 2.20 (1H, T*p*-H2′*), 2.49 (1H, T*p*-H2″*), 3.52 (3H, N^3-CH_3), 3.59 (2H, T*p*-H5′; H5″), 3.85 (2H, CH_2 7), 4.12 (1H, T*p*-H4′), 4.67 (1H, T*p*-H3′), 6.27 (1H, T*p*-H1′); 7.47 (1H, T*p*-H6); 8.42 (1H, -*p*TH6), ^{31}P NMR (D_2O) 26.76; *assigned only pairwise; FABMS *m/z* 465 $(M + Na)^+$, 443 $(M + H)^+$.

19: UV (λ_{max} H_2O) 265 nm; ^1H NMR (300 MHz D_2O) 1.74 (3H, d, J = 17.7, *p*-CH_3), 1.90 (3H, s, T*p*-CH_3*), 1.94 (3H, s, -*p*TCH_3*), 2.45 and 2.57 (3H and 1H, m, H2′, H2″ T*p*- and -*p*T), 3.29 (3H, s, N^3-CH_3), 3.78 (2H; m, T*p*-H5′, H5″), 4.18 (1H, m, -*p*TH4′), 4.25 (1H, m, T*p*-H4′), 4.34 (2H, m, -*p*TH5′, H5″), 4.58 (1H, m, -*p*TH3′), 5.09 (1H, m, T*p*-H3′), 6.23 (1H, t, J = 6.7, T*p*-H1′), 6.34 (1H, t, J = 6.4; -*p*TH1′), 7.54 (1H, s, -*p*TH6), 7.63 (1H, s; T*p*-H6); ^{31}P NMR (D_2O) 36.57 ppm; *may be interchanged.

20: UV (λ_{max} H_2O) 264 nm; ^1H NMR (300 MHz D_2O) 1.68 (3H, d, J = 17.6, *p*CH_3), 1.89 (3H, s, T*p*-CH_3), 2.40 (3H, m, -*p*TH2′ H2″ and T*p*-H2′), 2.55 (1H, m, T*p*-H2″), 3.24 (3H, s, N^3-CH_3), 3.73 (2H, m, -*p*TH5′, H5″), 4.14 (1H, m, -*p*TH4′), 4.21 (1H, m, T*p*-H4′), 4.30 (2H, m, -*p*TH5′, H5″), 4.32 (2H, s, CH_2 7), 4.53 (1H, m, -*p*TH3′), 5.03 (1H, m, T*p*-H3′), 6.19 (1H, t, J = 6.8; T*p*-H1′), 6.29 (1H, t, J = 6.3; -*p*TH1′), 7.50 (1H, s, -*p*TH6), 7.82 (1H, s, T*p*-H6); ^{31}P NMR (D_2O) 35.95 ppm; FABMS *m/z* 597 $(M + Na)^+$.

Acknowledgment. We are indebted to the Swedish Research Council for Engineering Sciences for financial support. We are grateful to D. Guillaume for a number of NMR spectra. We also thank J. Rossier and J.-P. Le Caer (Institut A. Fessard) for electrospray mass spectra and P. Varenne and C. Girard (Service de spectrométrie de masse, ICSN) for their assistance.

Abbreviations: Tps^{4}T, thymidylyl-(3′−5′)-4-thiothymidine; TpT, thymidylyl-(3′−5′)-thymidine; Tpm^{3}s^{4}T, thymidylyl-(3′−5′)-N^3-methyl-4-thiothymidine; T*p*m^{3}s^{4}T: 5′-N^3-methyl-4-thiothymidine 3′-(thymidinyl methylphosphonate). For the sake of simplification, in each dinucleotide phosphate or methylphosphonate, T*p*- refers to the 5′ terminal residue and -*p*T to the 3′ terminal residue.

Supplementary Material Available: Copies of ^1H NMR spectra of **11a,b**, **12b,c**, **13b,c**, **14b,c**, **15a,b**, **17**, and **18** (12 pages). This material is contained in libraries on microfiche, immediately follows this article in the microfilm version of the journal, and can be ordered from ACS; see any current masthead page for ordering information.